UNIVERSITY OF CALIFORNIA

SANTA CRUZ

UTILIZING ADVANCED TECHNIQUES IN NMR SPECTROSCOPY TO STUDY THE CONFORMATIONAL ASPECTS OF MEMBRANE PERMEABILITY FOR N-METHYLATED CYCLIC PEPTIDES.

A thesis submitted in partial satisfaction
of the requirements for the degree of

MASTER OF SCIENCE

in

CHEMISTRY AND BIOCHEMISTRY

by

Chad M. Renzelman

June 2012

The Thesis of Chad M. Renzelman
is approved:

_____
Professor William G. Scott, Chair

_____
Professor R. Scott Lokey

_____
Professor Scott R. J. Oliver

_____
Tyrus Miller
Vice Provost and Dean of Graduate Studies

Table of Contents

List of Figures

Abstract

Chad M. Renzelman

UTILIZING ADVANCED TECHNIQUES IN NMR SPECTROSCOPY TO STUDY THE CONFORMATIONAL ASPECTS OF MEMBRANE PERMEABILITY FOR N-METHYLATED CYCLIC PEPTIDES.

The conformational hypothesis of membrane permeability hypothesizes that certain macrocyclic scaffolds can exhibit an abnormally high degree of permeability producing a larger logP value than expected due to intramolecular hydrogen bonding which locks the macrocycle into a specific conformation where the hydrophilic functional groups are buried within the molecule causing it to become lipophilic enough to cross the membrane. Exploring this concept in previous work resulted in the synthesis of a 32 membered library of cyclic peptides with the same sequence varying in stereochemistry and N-methylation pattern. From this library two cyclic peptides, compounds 1 and 2 were found to exhibit an abnormally large logP value when assayed using the PAMPA permeability assay. This result lead us to synthesize more of these compounds and subject them to a series of NMR and other analytical experiments to computationally determine these two molecules 3D structure as they exist in chloroform solution, used to mimic the environment of the inside of membrane bilayer. These NMR structures were produced using NOESY derived distance restraints and the molecular modeling program CYANA. These structures provide valuable information about what types of conformational motifs can be used when designing novel therapeutic compounds.

Dedication and Acknowledgement

Special thanks are due to James “Jim” Loo the recently retired NMR Manager who taught me that all energy flows according to the whims of the great magnet.

White, T. R.; Renzelman, C. M.; Rand, A. C.; Rezai, T.; McEwen, C. M.; Gelev, V. M.; Turner, R. A.; Linington, R. G.; Leung, S. S. F.; Lokey, R. S.; . On-resin N-methylation of cyclic peptides for discovery of orally bioavailable scaffolds. *Nature Chemical Biology* **2011,** *7* (11), 810-817.

Background:

The devout acceptance by the western world of allopathic medicine[1], fueled by the research powerhouses of the pharmaceutical industry, makes the quest for novel therapeutic agents an exciting and enduring area of research[2]. The task of finding new drugs or novel therapeutic agents at times can seem more like a sophisticated art form than a precise science[3]. When trying to determine if a potential molecule is a good therapeutic agent or druglike molecule it can be very helpful to analyze the molecule in accordance to Lipinski's Rule of Five[4]. Lipinski's Rule of 5 is a set of conditions used to evaluate bioactive compounds on their "druglikeness" or their potential to become a good orally active drug[5]. These criteria are based on molecular properties that can affect the molecules pharmacokinetic profile, indicating how the molecule will behave while being metabolized by the body. These criteria can only predict pharmacokinetic properties and in no way can predict a molecule's bioactivity. The Lipinski's Rule of 5 is as follows:

- No more than 5 Hydrogen Bond Donors
- No more than 5 Hydrogen Bond Acceptors
- Molecular mass of no more than 500 g/mol
- an Octanol-Water Partition Coefficient, LogP Value no greater than 5

When looking at the criteria set forth by Lipinski's Rule it becomes clear what is required to make a molecule a good drug, it must not have an excess of hydrogen

bond donors or acceptors, it must be a reasonably small molecule and it must be able to partition across the cell membrane or the blood brain barrier. This limits many bioactive molecules from becoming good drugs either because they are too large or have too many hydrogen bond donors or acceptors. When looking at the molecular structures of the compounds that comprise the top ten list of pharmaceutical sales, we find that the overwhelming majority of them are classified as small molecules[6]. Natural products are another source of bioactive molecules that are often utilized as drugs[7]. Natural products are unique molecules made biosynthetically by living organisms and subsequently extracted and isolated by the scientist in the laboratory[8]. These molecules provide a rich diversity of structures and scaffolds that once explored will yield a treasure trove therapeutically relevant biologically active molecules[9]. One such natural product that proves to be very interesting is Cyclosporine. Cyclosporine is an immunosuppressant drug used commonly in organ transplants to prevent rejection of recently transplanted organs[10]. This molecule is large macrocylic polypeptide natural product originally isolated from the fungus *Tolypocladium inflatum*[11]. Cyclosporine $C_{62}H_{111}N_{11}O_{12}$ has a molecular weight of 1202.61 g/mol it has a total of 12 hydrogen

Figure 1: Cyclosporine

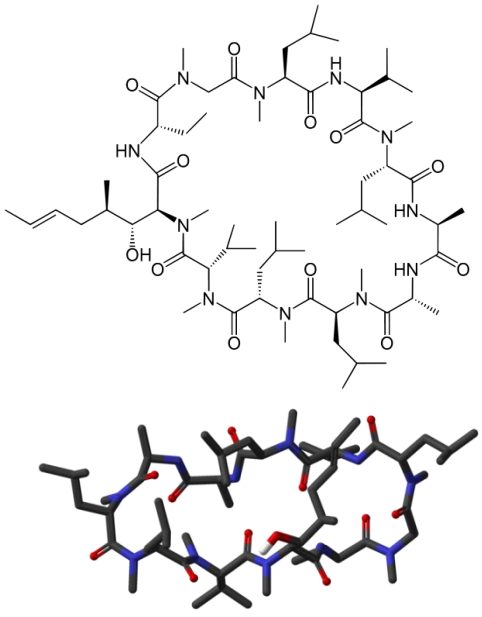

bond acceptors and 5 hydrogen bond donors and a LogP Value of 4.3[12]. If we were to evaluate Cyclosporine in accordance to Lipinski's Rules of Five we would find that all but one of Lipinski's rules are violated. Drawing from these results there stands little reason to believe that cyclosporine would be an orally available pharmaceutical compound, yet on the contrary, it is a commonly used pharmaceutical sold on the market[13]. There must be some aspect of this molecule that confers pharmacokinetic properties allowing this seemingly poor "druglike" molecule to be a good orally active pharmaceutical. Cyclosporine has seven N-methylated backbone amide nitrogen atoms conferring rigidity to the macrocyclic ring structure. The N-methylation of backbone nitrogen atoms not only provides a great degree of stability to the macrocycle but at the same time, it also increases its bioavailability by preventing enzymatic degradation of the amide bond[14]. The pharmacokinetic properties gained through N-methylating the amide backbone of Cyclosporine allows it to be a good drug despite its large size and excessive hydrogen bonding[15].

Macrocyclic molecules have gained a lot of recent attention as potential scaffolds for development of novel bioactive therapeutic agents that could potentially yield new and exciting treatments for a myriad of diseases[16]. Macrocyclic compounds such as cyclic peptides are an exciting class of organic molecules[17]. Due to the inherent variability achieved by being a polypeptide coupled with distinct tertiary conformations achieved through cyclization makes cyclic peptides very appealing as potential drug candidates[18]. Cyclic Peptides have the ability to form

unique and interesting tertiary conformations that allows them to interact with biological targets in a variety of different ways drastically increasing the selectivity and specificity of these molecules as compared to small molecule drugs that commonly interact with only one active site[19]. Cyclic peptide motifs are often found in bioactive molecules that are derived from marine natural products[20]. The natural product molecules were biosynthetically produced from the symbiotic relationship

Figure 2: Cyclic Peptide Natural Products

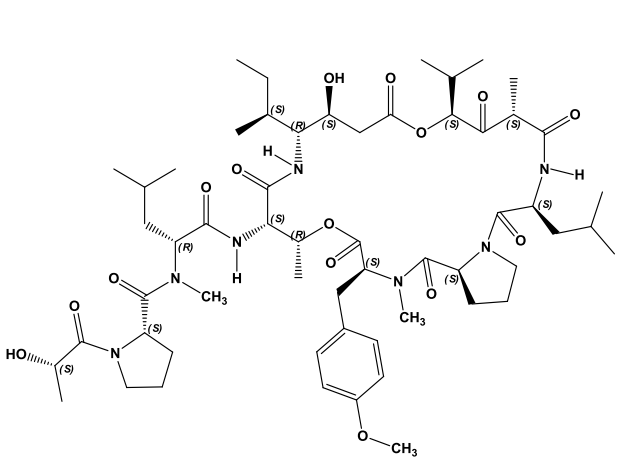

Didemnin B

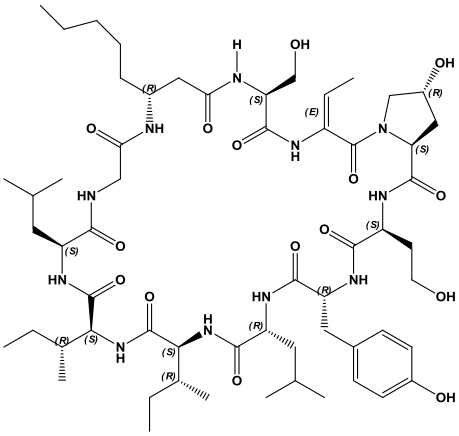

Lobocyclamide A

between tropical marine sponges and a variety of microbial flora and fauna (bacteria and fungi) found living within the body of the sponge[21]. This poorly understood relationship has yielded a plethora of biodiversity in natural products that can be utilized by clever scientists to find a veritable goldmine of new molecules that could potentially be honed into new therapeutic agents[22]. Some examples of bioactive natural products that are classified as cyclic peptides are shown in Figure 2. Both of

these molecules are macrocycles constructed out of amino acid residues and then cyclized to form a macrocyclic ring structure. The ring closure can be accomplished by two different methods. The classic head to tail cyclization where the N-terminal amino group forms an amide bond with the C-terminal carboxylic acid, as is the case in Lobocyclamide A shown in Figure 2[23]. The second motif involves cyclizing through the formation of an ester linkage between the carboxylic acid of the C-terminus and an alcohol side chain of either a serine or threonine, in the case of Didemnin B the side chain is a threonine residue as seen in Figure 2[24].

The cyclization of peptides is beneficial to the development of these molecules as potential drugs due to the increased pharmacokinetic properties achieved through cyclization. Cyclizing a linear peptide significantly reduces the enzymatic degradation of the molecule in the blood stream increasing the half-life of the molecule[25]. Since peptides utilize the amide bond, they are susceptible to enzymatic degradation in the blood stream[26]. This makes it difficult to use natural peptides as potential drugs since they are easily degraded and

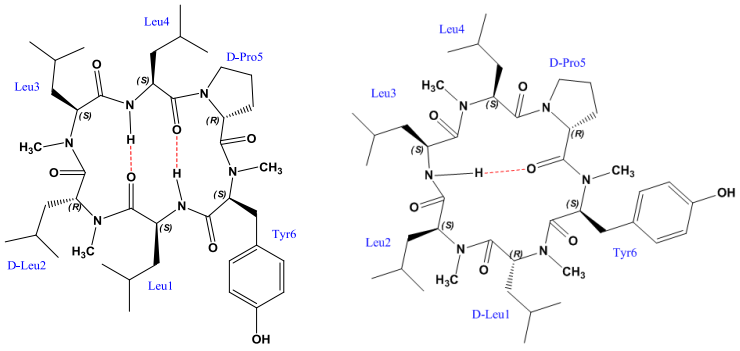

Figure 3: 2D Structures of Compounds 1 and 2

removed from the bloodstream[27]. To overcome this problem we have chosen to use cyclic peptides as the focus of research for this thesis.

Ongoing research in our lab has produced many different cyclic peptides varying in length, sequence and backbone amide methylation[28]. The two molecules that will be focused on in this thesis will be referred to as 1 and 2 the structures of which are shown in Figure 3. Compound one is the tri-methylated peptide and two is the tetra-methylated species[29]. The structures shown in Figure 2 illustrate the hydrogen-bonding pattern of the two molecules by using a red dotted line to represent the hydrogen-bonding event taking place transannularly across the ring from the electron pairs on the carbonyl oxygen to the proton of the amide nitrogen. Compounds 1 and 2 have differing hydrogen-bonding patterns due to the molecules having different sequence stereochemistry at the Leucine amino acid side chains, along with the different N-methylation pattern of the backbone amide nitrogen atoms. The difference in N-methylation pattern gives the molecules differing numbers of hydrogen bond donors due to the proton on the amide nitrogen. It is the 3D conformations of these molecules produced by transannular hydrogen-bonding that makes these molecules particularly interesting. According to Lipinski's Rules cyclic peptides of this type would not be considered good druglike molecules and most certainly would not be considered membrane permeable[30]. The transanular hydrogen bonding allows the molecule to afford a conformation that effectively shields its hydrophilic functionalities by locking them in a hydrogen-bonding event. This allows

the molecule to become quite lipophilic giving it access to cross the cell membrane or the blood brain barrier, making these compounds surprisingly "druglike"[31]. Extensive testing in our research laboratory on bioactive molecules and membrane permeability lead us to two interesting scaffolds (1&2) that proved to be very permeable despite their somewhat cumbersome attributes. These discoveries helped to formulate the conformational hypothesis of membrane permeability.

Figure 4: Conformational Hypothesis of Membrane Permeability

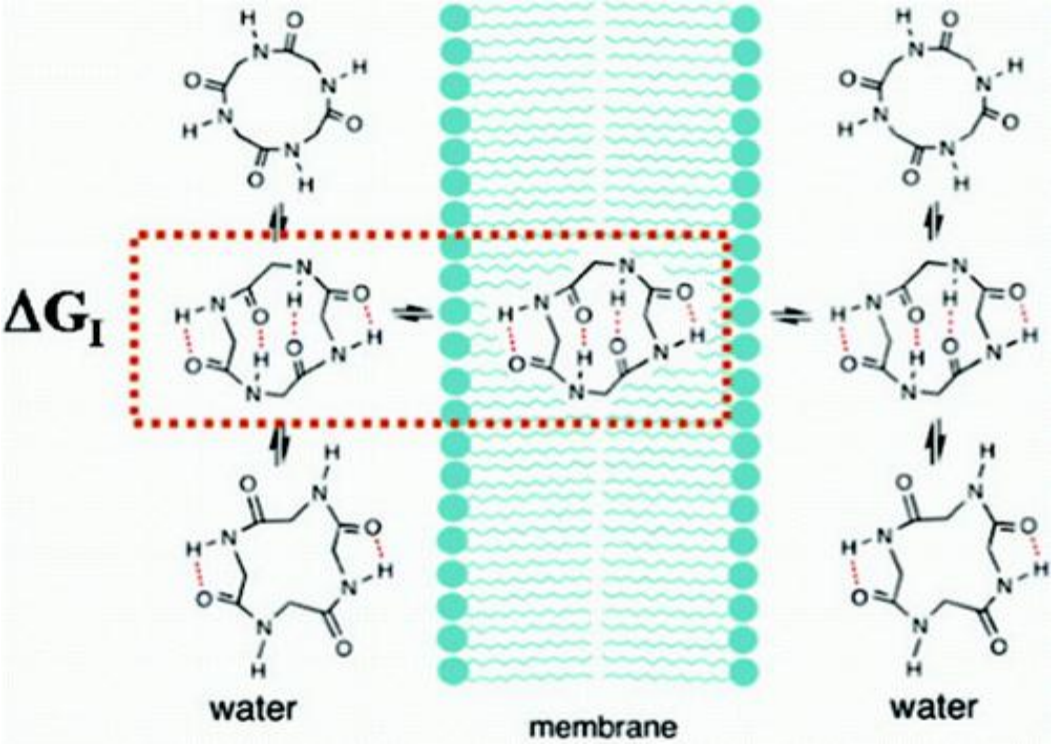

The conformational hypothesis of membrane permeability is a hypothetical model that is used to explain the membrane permeability exhibited by certain

molecules that ordinarily would not be permeable under the observed conditions. Conformational shifting of these molecules allows them to bury the hydrophilic functional groups by locking them into a hydrogen-bond. This allows the molecule to become effectively hydrophilic allowing it to passively diffuse through the membrane. This concept is outlined in Figure 4[32]. In solution phase the cyclic peptide affords many different conformations allowing the hydrogen bond donors and acceptors to become involved in hydrogen bonding events transannularly as well as amongst the water molecules present in the solvent, thus causing the molecule to sample all of the many different conformational positions available to it in space-time. There is one particular conformation that is achieved when the molecule is in a solution that has a low dielectric constant, such as the membrane. This conformation hides all of the hydrophilic portions of the cyclic peptide by involving them in intramolecular hydrogen bonds causing the molecule to effectively bury the hydrophilic portion in the interior of the molecule leaving the lipophilic portions exposed. This allows the molecule to slip into the hydrophobic interior of the membrane. Once the molecule has left the membrane it is once again free to explore all possible conformations allowed to it by the fundamental laws of physics. This is the essence of the conformational hypothesis of membrane permeability.

Cyclic peptides are very interesting molecules to study due to the unique 3d conformations that they can assume in the solution phase. These conformations can differ depending upon the properties of the chemical environment experienced by the

cyclic peptide; such as the dielectric constant, viscosity, and temperature of the solvent molecules[33]. Studying these different conformations and how they change in varying dielectric constants can provide great insight into the mechanism that is used by these cyclic peptides to passively diffuse through the cell membrane. Insight into this mechanism will only help fundamentally advance the science of new drug design allowing scientists to custom design large macromolecules that specifically bind to the target biomolecule through multiple interactions around the target. This allows the pharmaceutical chemist to design new drug therapies that are extremely selective thus severely reducing side effects by eliminating off target interactions. In order to advance to that state of pharmaceutical design we must devise a set of tools that will allow us to look at these molecular conformations in solution[34]. X-Ray Crystallography is an immensely powerful tool that can precisely determine a molecules regiochemistry and absolute stereochemistry at angstrom level resolution, but one must freeze the molecule into a crystal lattice of superb quality in order to get good resolution[35]. This process can become very challenging and take entire careers to obtain a single crystal[36]. Crystallographic technique aside, once obtained, the diffraction pattern gives you clear results of an inherently false image. Locking the molecule into a crystal lattice freezes the molecule into a conformation that exhibits the lowest free energy ΔG. The conformation achieved by the crystal may or may not be the biologically active conformation[37]. This limitation forces us to resort to other spectroscopic techniques that can performed on the molecule while in solution,

allowing the scientist to vary conditions such as pH, polarity, temperature and dielectric constant, all of which can drastically affect the 3d conformation of the molecule[38]. The desire to analyze these compounds in solution and obtain structural information about the molecule makes nuclear magnetic resonance the ideal analytical technique for the job at hand[39].

Recent advances in the field of nuclear magnetic resonance has yielded the development of a plethora of new and exciting pulse sequences that provide the analyst with a veritable toolbox from which one can probe almost any question imaginable[40]. Hydrogen-Deuterium exchange experiments with cyclic peptides can determine whether any particular amide protons are involved in a hydrogen bond or just exposed to the solvent[41]. 2D NMR techniques such as COSY, TOCSY, HMBC, HSQC, ^{1}H, and ^{13}C are used to accurately determine the molecules structure, regiochemistry and stereochemistry[42]. One of the most important breakthroughs in the field nuclear magnetic resonance spectroscopy was the discovery of the Nuclear Overhauser Effect (NOE)[43]. The steady-state nuclear Overhauser effect arises throughout the RF saturation of one spin; the effect will cause perturbations in the spins of neighboring nuclei via dipolar interactions effectively enhancing the intensity of the neighboring spins. Since dipolar couplings can readily interact through space, this makes NOE spectroscopy an extremely useful tool for the conformational study of molecules.

The pulse sequence for the two dimensional NMR experiment Nuclear Overhauser Effect Spectroscopy (NOESY) is clearly illustrated in Figure 5[44]. The first pulse equalized the population differences across all energy levels. Coherences then evolve during the τ_1 period thus encoding the phase in the second dimension. The second pulse transfers magnetization of all the spins back to the Z direction enabling the mixing. The NOE is evolved during the mixing time τ_m which must be

Figure 5: Pulse Sequence for the 2D NOESY Experiment

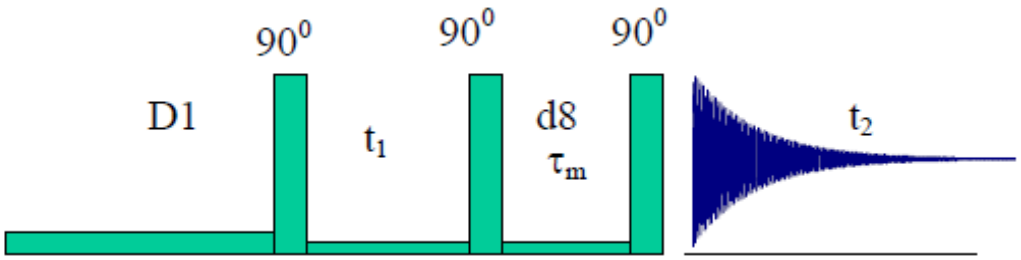

chosen carefully for each specific molecule. The last pulse converts the mixed magnetization to the xy plane rendering the NOE signals ready for observation. The spectra is phased and depending upon the molecular mass of the compound and the rate at which it tumbles, the spectra can be phased either negatively or positively yielding a two dimensional spectra whose cross peaks represents the distance through space between the two nuclei[45]. This data can be calculated into angstrom distances and used as distance constraints in molecular dynamics simulations which can produce accurate three dimensional models of the compounds as they would look in

solution in the NMR tube. This is done by integrating the cross peaks of the 2D NOESY spectra and carefully measuring the area of the peak. The peak area is converted to distance in angstroms (Å) using the formula shown in Figure 6[46]. V_x stands for the peak volume of the integrated cross peak and Vref stands for the peak

Figure 6: Equations for NOESY peak area to distance calculation

$$\frac{V_x}{V_{ref}} = \frac{d_x^{-6}}{d_{ref}^{-6}} \qquad V_x = V_{ref}\frac{d_x^{-6}}{d_{ref}^{-6}}$$

volume of the reference peak which is usually a set of diastereotopic protons found on the molecule. The distance (d_x) in angstroms is the through space interproton distance representing the space between the two nuclei in the spin systems. The distance (d_{ref}) is the known distance between two germinal protons attached to the same carbon atom. This distance is used as the reference set for the experiment. With this information one can create a nice set of distanced restraints that accurately represent the conformation of the molecule as captured at the time of the NMR experiment. This set of distance restraints is then used as input data along with the sequence information in a molecular dynamics simulation, which uses advanced algorithms to produce accurate 3D representations of the cyclic peptide as it looks according to the calculated distance restraints[47]. This is how one can use advanced

NMR techniques to visually image the bioctive moleucle in three dimensional space, accurately detailing the conformational nuianses that make these macrocycles such interesting and majestic compounds. Not only can we visualize these molecules as they exist in solution at a given dielectric constant but we can take a snapshot in time and capture an interaction or conformation that may occur in a fleeting moment but is till able to be measured on the NMR timescale. In a narcassitic grasp for meaning this technique is somewhat like a type of molecular cinema camera documenting the gritty beach reality show that is the moelcular pharmacetical world, providing a quick glimsp, albeit airbrushed to perfection, into an otherwise unforseeable plane of existence. One example of a 3D model representation of a cyclic peptide that was created using distance restraints obtained from integrating NOESY experiments and then subsequently entered into molecular dynamics simulations to produce the structure shown in Figure 7. This clearly shows the conformation exhibited by

Figure 7: 2D and 3D model of the Cyclic Peptide Compound 1

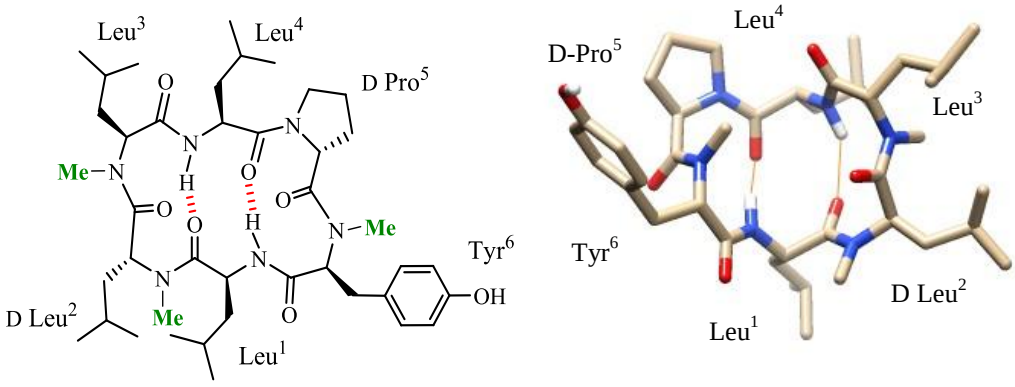

Compound 1 **Compound 1**

compound 1 in solution dissolved in chloroform (dielectric constant = 4.8) which is very close to that of the interior of the cell membrane (dielectric constant = 9) as compared to water (dielectric constant = 80) which is considerably higher[48]. This is the conformation achieved by the molecule that allows it to passively difffuse through the cell membrane, it exhibits a low energy well and shows some very important chracteristics. These charcterics include the transannular hydrogen bonds locking the macrocycle into its characteristic low energy conformation where the hydrogen-bond donors and acceptors are occupied by intramolecular hydrogen-bonding thus burying the hydrophillic functional groups in the molecule leaving the hydrophobic or lipophilic functional groups exposed thus fascilitating the passive diffusion through the cell membrane[49]. Visualizing this conformation thorugh advanced NMR and computational chemistry techniques has allowed us to understand the structural and conformational basis for this molecules membrane permeability. Understanding into the relationships between conformational structure and the molecules inherent membrane permeability via passive diffusion can provide great insight into structure activity relationship studies of new scaffolds and basic themes for advanced molecular design of new bioactive compounds which will be used as lead targets in pharmaceutical screening protocols[50].

Upon anlysis and computation of the NMR data one is left with a set of intermolecule distances through space in a molecule in solution. These distance restraint must then be used in a separate computation where the program inputs the

distance restarints along with known geometrical parameters of the cyclic peptides sequence, and uses this information to construct and anneal the molecule into a three dimensional conformation showing how the molecule exists in space[51]. There are are a variety of different methods from which one can calculate the structure of these cyclic peptides from NMR derrived distance restraints. Once the distance restraints have been calculated the next step is to decide how to proceede with the structure calulation. Most molecular structures are represented using the .pdb or protein data bank file format which is a textual file format describing the three dimensional structure of molecules held in the protein data bank (www.wwpdb.org)[52]. These files are readily viewed by a number of viewing programs the such as pymol[53] and UCSF Chimera. UCSFChimera is an extensive molecular modeling system supplied by the fine folks at the University of California San Francisco, this program was the viewing software used in this thesis which allows one to view and manipulate the structure in 3D space and is responsible for such fine work as Figure 7[54]. These programs that were so kindly benefacted by the great educational instution UCSF, privy the scientist to an otherwise undiscoverable world. They allow us insight into these molecules that can not be matched. With such vivid visualization of these bioacitve molecules the pharmaceutical chemist can really become one with the active pharmaceutical ingredients. These programs allow us to visualize the cyclic peptides that we are interested in but it takes another process entirely to produce the coordinates that are being viewed by the UCSFChimera program.

There are a few different computational methods used to calculate the structure coordinate file (.pdb) but in all cases they take two separate input files, a sequence file outlining the amino acids in the peptide and thier appropriate order in the sequence, and a distance restraint file detailing the calculated distances from the NMR data. These two data sets are used to calculate the structure of the cyclic peptide, the algorythm used can vary depending on the software that is used. The software system that was used in this thesis is CYANA created by Professor Dr. Peter Güntert at the University of Frankfurt[55]. This program allows the user to input sequence information along with the NMR derived distance restraints as the input files. The program then uses a system of simulated annealing, varyinng the temperature in the simulation allows for the fast exploration of conformational space with torsion angle dynamics[56]. This allows the program to overcome local minima to produce a reliable three dimensional structure. The advances in science that this technology represents will drastically advance the way scientist design and produce pharmaceutical compounds.

The analysis of these cylcic peptides to produce accurate three dimensional representations of the cyclic peptides in solution provides great insight into the mechanics of the conformational hypothesis of membrane permeability. The ability to visualize these macrocyclic ring structures as they exist in solvents of varying dielectric constants really allows the chemist to design novel bioactive molecules that interact with any number of targets both strategically and most importantly

selectively. This technology coupled along with recent advances in X-ray crystallography techniques will most certainly revolutionize pharmaceutical science as we know it today.

Experimental Design: Previous work in our lab synthesizing cyclic peptide libraries has produced a great number of cyclic peptide scaffolds that have the same linear sequence but differ in the stereochemistry of each residue in the sequence (d or l amino acid). The linear sequence before cyclization in the standard N-terminus to C-terminus notation is Leu-Leu-Leu-Leu-dPro-Tyr. Varying the positions in which dLeu is substituted for Leu produced a library of 32 cyclic peptides[29]. Two cyclic peptides were chosen as the subjects of analysis for this thesis, compound 1 and compound 2 which are shown in Figure 3 and have the linear sequences of Leu-dLeu-Leu-Leu-dPro-Tyr for compound 1 and dLeu-Leu-Leu-Leu-dPro-Tyr for compound

Figure 8: Schematic of the PAMPA Permeability Assay

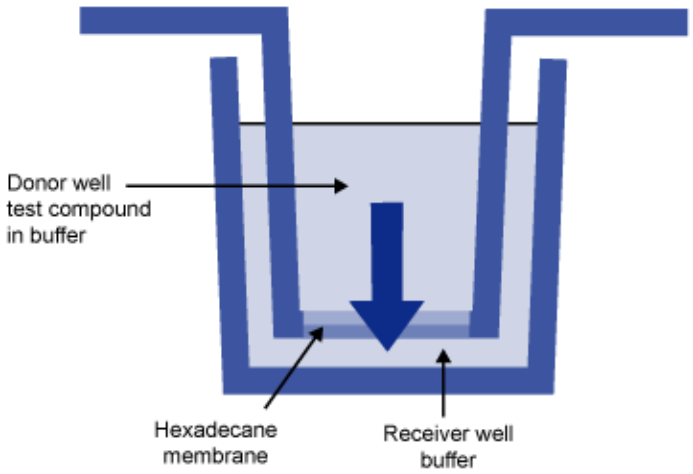

2. These cyclic peptides were chosen because they exhibited a high degree of membrane permeability when assayed using the PAMPA parallel artificial membrane permeability assay, which was used to determine the Log P values of the cyclic peptide library. Out of the library of 32 different cyclic peptide scaffolds two compounds, 1 and 2 were the only peptides that could passively diffuse through the

Figure 9: Synthetic Scheme for Compounds 1 and 2

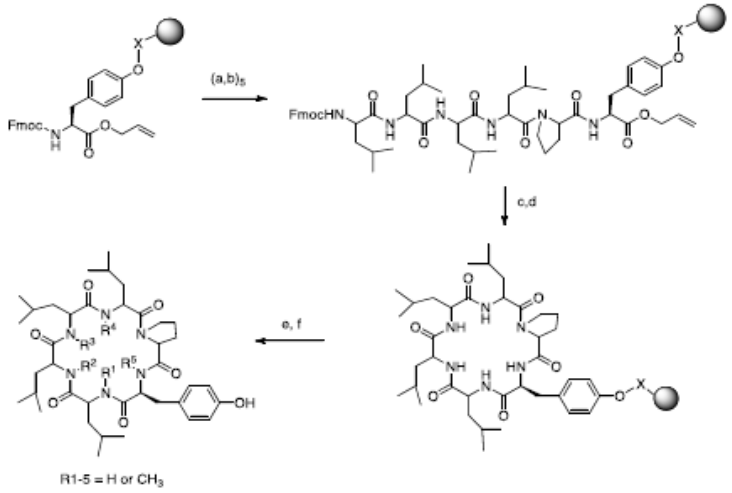

Scheme S1. Synthetic scheme for solid phase synthesis and on-resin N-methylation of cyclo[Leu, Leu, Leu, Leu, Pro, Tyr]. X = all-alkyl diisopropyl silyl resin. Conditions: (a) 20% piperidine(v/v) in DMF; (b) Fmoc-aa-OH, HBTU, DIEA, DMF; (c) $Pd(Ph_3P)_4$, piperidine (10% v/v), THF; (d) PyBOP, HOAt, DIEA, DMF; (e) base, additive, CH_3I (see Table 1). (f) 5% HF/py in THF.

artificial lipid membrane of the PAMPA plate. This result intrigued us and we decided to probe the conformational aspects of these molecules to see what was allowing them to become membrane permeable. With this goal in mind we set forth

to synthetically produce enough purified material of both compounds, in order to subject them to a vast number of analytical techniques. The linear peptide precursor of the cyclic peptides was constructed by using a Prelude peptide synthesizer utilizing SPPS solid phase peptide synthesis techniques. The synthesizer automates all of the coupling reactions by automatically dispensing the appropriate chemicals and allowing them to mix for the appropriate reaction times and finally washing the resin in between couplings with clean solvent, yielding the completed linear peptide deprotected but still on the resin. The linear peptide was then cyclized head to tail on the resin to form the cyclic peptide. The purified cyclic peptide was then subjected to

Figure 10: Hydrogen-Deuterium Exchange Data

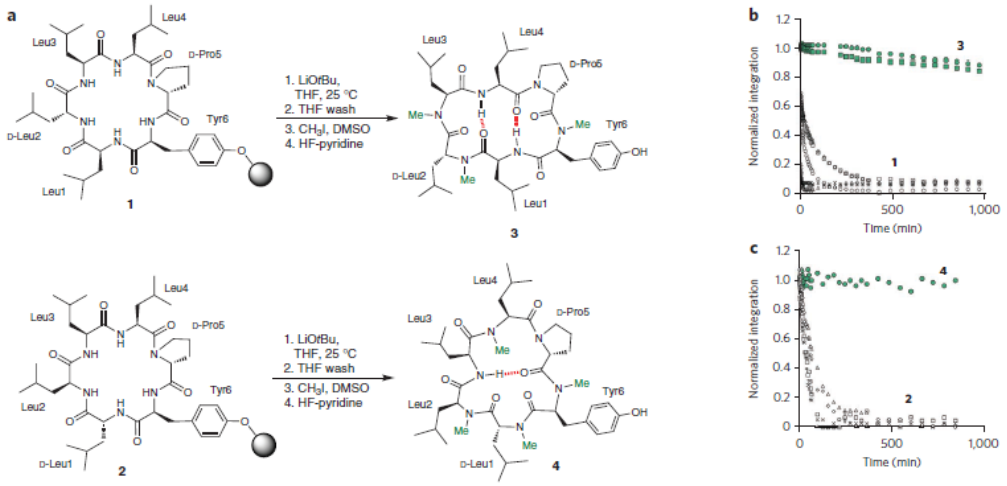

Figure 3 | Most selective scaffolds, their N-methylation products and H-D exchange studies. (**a**) Reaction sequence in the on-resin N-methylation of **1** and **2** and the resulting pattern of alkylation that generates **3** and **4**, respectively. (**b**,**c**) H-D exchange studies on **1** and **3** (**b**) along with **2** and **4** (**c**). Amide N-H resonances were monitored as a function of time after addition of 5% methanol-d_4 (*v*/*v*) in 0.5% acetic acid-d_4. LiO*t*Bu, lithium *tert*-butoxide.

methylating conditions deprotonating the amide proton causing it to react with methyl iodide in a S_N2 reaction to yield the N-methylated amide bond. Upon completion of the methylation reactions, we have the finished cyclic peptide still attached through

the tyrosine side chain to the solid resin beads. At this point, the compounds were cleaved from the resin with strong acid and subsequently precipitated with ether to remove all traces of the acid before further purification. The compounds were then purified using a Shimadzu preparatory scale HPLC high-pressure liquid chromatography system using a reverse phase C18 solid phase column. The product was then reconstituted from the aqueous solution by flash freezing with liquid nitrogen and subsequently subjected to lyophilization to yield a fluffy white powder.

Once synthesized and purified, compounds 1 and 2 were then subjected to a number of analytical techniques to learn as much as possible about the structure and conformation of these molecules. A number of different NMR techniques were used to characterize these molecules. The first step in calculating the final structure of a compound is the assignment of all atoms in the molecule to their corresponding resonances in the NMR spectra. This was done by running the full gambit of the standard 1D and 2D NMR experiments, such as ^{1}H, ^{13}C, TOCSY, COSY, HMBC, and HSQC. These spectra were used to determine the position of each atom in the molecule and assign to it an exact resonance peak in the NMR spectra, providing that the atom has an odd number of protons and neutrons[57]. Complete assignment of all resonances to their corresponding atomic nuclei is absolutely necessary to perform the structure calculation. In order to determine where a particular atom is in three-dimensional space, you must first know its position in the molecule. This was accomplished by assigning the corresponding resonance peak in the NMR spectra to

the atom the molecule that is responsible for it. Doing this gives us quite a bit of information about the molecules. Through total assignment, one can tell which amino acid in the compound is N-methylated. Mass Spectrometry can tell us how many amino acids were methylated but will not provide any positional information. One must run the HMBC and HSQC NMR experiments in order to accurately assign the methyl groups on the backbone of the cyclic peptide which is illustrated is Figure 11.

Hydrogen-Deuterium exchange experiments were performed to see which amide protons are in hydrogen-bonding environments, since the amide protons are the only exchangeable protons other that the phenol on tyrosine. The protons that are involved in a hydrogen-bonding event will exchange less readily/rapidly with the deuterium atoms present in solution, while the protons that are not involved in a hydrogen bond or are exposed to solvent do exchange very quickly. By measuring the rate of exchange with deuterium atoms of the amide protons in the cyclic peptide once can deduce whether a proton is involved in a hydrogen bond or not[58]. Since hydrogen bonds have characteristic distances (1.97 Å), this exchange data can provide valuable conformational information about these compounds[59].

The last NMR experiment that was performed on compounds 1 and 2 was the 2D NOESY experiment. We proceeded with this analysis to extract structural information about the molecule from the integrated resonance peaks developed during the NOESY experiment. The resonances were integrated and the volumes used to

calculate interproton distances within the molecule, that were subsequently used as a set of distance restraints in a molecular dynamics program that produced the final structural model. Constructing a three dimensional model of a compound in solution

Figure 11: Illustration of interatomic correlations found in 2D NMR experiments

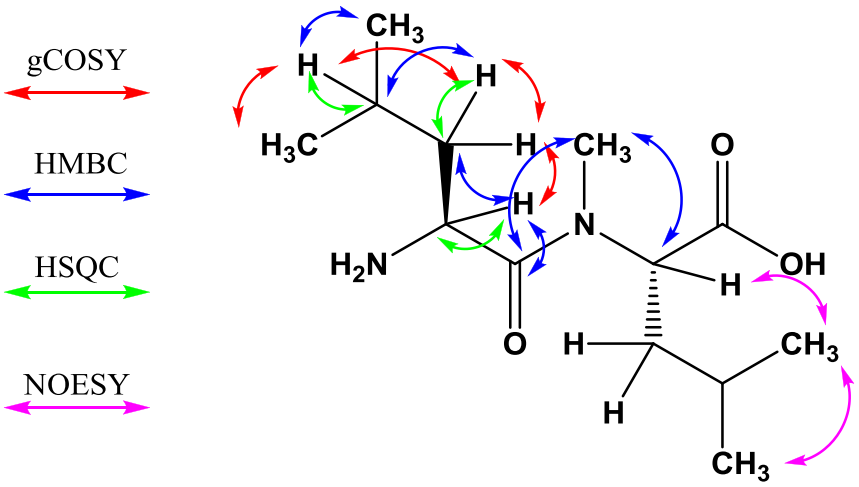

can be a very challenging task. The right combination of analytical experiments is required to provide valid conformational data about the molecule. This data is used in concert with computational techniques to produce a tangible model of the compound, *in silico*, that can be used to study many aspects of pharmacology and chemistry[60]. The next few paragraphs will be focused on outlining the fundamental procedure of constructing the final NMR solution structure of compounds 1 and 2, laying out the steps in such a fashion that one could follow them from beginning to end in one comprehensive set of experimental concepts and procedures.

Once the compounds were synthesized and purified, the first step in the procedure was to prepare the sample for NMR analysis. This was done first to ensure

that the sample was free from impurities, water, or product degradation material. The sample was then kept under reduced atmosphere in a desiccator attached to a high performance vacuum pump for a minimum time of 24 hours, in order to ensure the complete removal of all water from the sample. This step is imperative to ensure the absence of a water peak in the NMR spectra that can obscure the data. Once the sample was completely dry it was dissolved in 100% deuterated solvent ($CDCl_3$) obtained directly from a sealed glass ampule and placed into an 8mm NMR tube that has been drying in the oven for no more than 40 minutes (to avoid warping the tube). The sample was then taken to the NMR room and subjected to the entire barrage of experiments to obtain a complete set of data for the compound. All possible NMR experiments should ideally be run consecutively on the sample without removing it from the NMR tube. Removal of the compound introduces water and impurities to the sample, which is an inevitable part of transferring compounds and should be avoided at all costs. The experiments that must be run on these compounds to determine the 3D structure as a follows; ^{1}H, ^{13}C, gCOSY, TOCSY, HMBC, HSQC, and NOESY or ROESY (depending of molecular mass of the compound). The initial six experiments were used to accurately assign the specific resonances to each atom in the compound, so when the NOESY spectra was obtained, it could be seen which atoms correlated to one another's magnetic spins through space. The correlations between the atoms produce resonances in the NMR spectra differently depending upon the pulse sequence used in the experiment. The correlations that are observed in

the various NMR experiments' spectra are illustrated visually in Figure 11 where each arrow shows the correlation represented by a cross peak spot on the 2D NMR spectra. The 1D ^{1}H and ^{13}C NMR spectra produce peaks that relate to every proton and carbon in the molecule experiencing a different chemical environment, while the 2D NMR spectra produce cross-peak spots that represent a correlation between two atoms in the compound; this correlation can represent different atomic interactions depending upon the pulse sequence and the experiment. These correlations were analyzed in order to piece together the resonances assignments with the compounds atomic structure, assigning each resonance to its corresponding atom. Once the assignments were made they were compiled into a data table for further scientific use, compound 1 has its NMR assignments shown in Figure 13 while compound 2 is shown in Figure 14.

The next step was to find the NOESY spectra with an appropriate mixing time τ_m that lies within the compounds' linear range as determined by creating a NOE build-up curve[61], to ensure that the peak volumes measured from the spectra can be calculated to determine interproton distances between the two protons responsible for the NOESY cross peak. The NOESY spectra were referenced to the solvent peak $CDCl_3$ and all of the cross-peaks (spots) were integrated and compiled into a table of integration values listing the peak volumes for

Figure 12: Proline

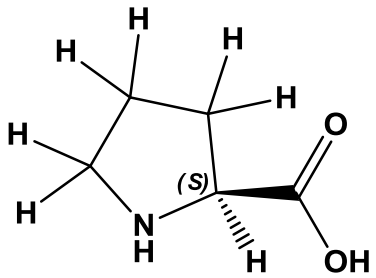

every resonance in the spectra. One very important resonance must be found before the distances can be calculated. This resonance is the reference peak, usually a pair of diastereotopic protons; two protons on a single carbon atom that give different resonance signals in the NMR spectra because they experience different chemical environments. The reference signal must be cleanly separated from all other peaks so an accurate integration value can be obtained. This can prove to be difficult with diastereotopic protons whose chemical environments are often very similar in nature. Great care must be taken to select and accurately integrate the reference signal as all the distance calculations are fundamentally based on the ratio of the reference signals peak volume to the known distance between the two protons. Since they are located on the same carbon atom the exact distance was known relating the volume of the integrated cross-peak to an exact interatomic distance in angstroms. The equation of this ratio is shown in Figure 6, this equation relates the integrated peak volume to distance by the inverse sixth power. This is usually done by choosing the diastereotopic protons on the heterocyclic ring structure of the amino acid Proline as seen in Figure 12. This is usually the preferred choice since the interproton distances for all of the diastereotopic protons pairs are known from X-Ray crystallography data[62]. Once the distances were calculated they were then compiled in an input text file and used as input data for structure calculation with the program CYANA.

CYANA was the molecular modeling software program used to create the (.pdb) file representing the 3D structure of the compound in a solution of

deuterated chloroform (ε_r 4.8) whose dielectric constant is similar to that of the inside of a cell membrane(ε_r 6)[63] as compared to the much higher dielectric constant of the very polar water molecule (ε_r 80.1)[64]. This was done by creating a few different input files that supply the program with all the necessary information for the structure calculation and simulated annealing. All of the files used in conjunction with the CYANA program are merely text files that were created with any simple text-editing program (such as Textwrangler)[65], samples of all the input and macro files discussed herein can be found at the CYANA-Wiki (www.cyana.org). The Cyana-Wiki provided a bountiful reference for all of the formatting and scripting information that was required to create all of the appropriate text files needed to execute the calculation. The first input file to be made was the sequence file (.seq); this file tells the program which amino acids residues are present in the peptide, and also calls up a list of atoms associated with the residues from the library file (.lib) already loaded with the program providing the general coordinates for each amino acid. If one needs to use non-natural amino acids or other such structures, the (.lib) library file must be modified with the proper distance coordinates for the new structure. Instructions for library file modification can be found at the CYANA-Wiki (www.Cyana.org). The next files made were the distance restraint files. The calculated distances obtained from the NOE data were converted to distance restraints by adding and subtracting 10% of the calculated distance for the upper and lower limits respectively. They were then saved as upper (.upl) and lower (.lol) distant restraint files using the text-editing

program, these files simply list the first atom followed by the second atom and then the distance restraint in angstroms. When available, coupling constant data can be converted to torsion angle restraints using the Karplus equation[66]. The calculated restraints were then saved as a torsion angle restraint file (.aco). Once all the distance restraint files were created, they were saved and placed together in a common folder. With the restraint files in place , the macro files were created giving CYANA all the names and locations of all the restraint files along with instructions about how many conformations to calculate, what sequence file to use, and the name and location of the output file (.pdb). The macro files used were the initialization macro file (init.cya) and the structure calculation macro (calc.cya) examples of each can be found at the CYANA-Wiki. Upon completion of all the files, the structure calculation is as simple as typing in a few commands into the terminal. The access to the X11 terminal is why the Macintosh G5 computer was used to perform all of the CYANA calculations. The commands needed to initiate CYANA begin by using the terminal to navigate into the file folder that contains the appropriate input and macro files created for the specific compound being analyzed. Once in the appropriate folder the CYANA program was started by typing CYANA and hitting the enter key. At this point the program will automatically read and launch the (init.cya) macro which initializes and loads the library (.lib) file along with the sequence (.seq) file. From here, the only thing left is to execute the calculation macro and consecrate the calculation. Once complete, the program writes a series of files to the hard drive. One is the structure

file (.pdb) containing the instructed number of conformations predetermined in the calculation macro. Other files produced along with the structure, are the text files outlining any abnormal violations of standard distances and dihedral angles that may help determine the overall quality of the model. This is how the model seen in Figure 7 was produced *in silico*. Now we are left with the most titillating moment of the procedure. Where up until now the unassuming file icon associated to the viewing program along with its file name is the only thing we know about the molecules structure. The brief moment of anticipation before the output file it is opened by the molecular modeling program (Chimera), thus revealing the immaculate structural beauty of the molecule in its three dimensional form, which was previously unseen by humankind, that is until now.

Experimental Procedures:

Synthetic Procedure for the preparation of compounds 1 and 2: Compounds 1 and 2 were synthesized using the technique of (SPPS) solid phase peptide synthesis[67]. The cyclic peptides were synthesized starting with the allyl ester of fluorenylmethyloxycarbonyl chloride (FMOC)-protected Tyrosine residue that was linked to the resin through its side chain as a silyl ether via the phenolic hydroxyl group to an all alkyl silyl tethered polystyrene resin. (4-methoxyphenyl) di-isopropylsilyl resin (Novabiochem, 0.71g, 0.994 mmol, loading 1.4 mmol/g) was treated with 6 equivalents of (DCM) under inert atmosphere in a flame dried 500 mL

round bottom flask for 1 hour. The solution was decanted via cannula and the resin was rinsed once with dry DCM. Fmoc-Tyr-OAllyl (0.88g, 1.988mmol) was then dissolved in a minimum amount of dry DCM obtained from the solvent still and added to the resin with 8 equivalents of 2, 6-lutidine (0.922ml, 7.952mmol), all done via cannula transfer utilizing a schlenk line.

The resin loading value was determined by UV-Vis spectroscopy using a small sample (13mg) of preloaded resin, treated with 1ml of a 20% piperidine/DMF solution, which cleaves off the Fmoc protecting group. The cleavage solution was collected, sub-diluted, and placed into a cuvette to prepare the sample for analysis. A wavelength of 301nm was used to measure the absorbance of Fmoc in a 1:100 dilution of the cleavage solution. The concentration of Fmoc in solution and the subsequent resin loading, could then be determined through Beer's Law[68], using an extinction coefficient of 7800. The resin loading value was determined to be 0.8 mmol/g.

Compounds 1 and 2 were synthesized and cyclized on resin using the Fmoc-Tyrosine loaded resin on an automated peptide synthesizer (Prelude, Protein Technologies)[69]. The coupling reactions creating the amide bond linkage between the two amino acid residues was achieved by adding 4 equivalents of Fmoc-protected amino acid, 3.8 equivalents of HBTU (*O*-(benzotriazol-1-yl)-*N*,*N*,*N*′,*N*′-tetramethyluronium hexafluorophosphate) and 6 equivalents of *N*,*N*-diisopropylethylamine (DIPEA) in dimethylformamide (DMF) for 1.5–3 hours. The

Fmoc deprotections were carried out with 2% diazabicycloundecene (DBU) in DMF for 15 min. After each coupling and deprotection step, the resin was washed with DMF (3 times), dichloromethane (DCM) (3 times) and DMF (3 times). After the addition of the final residue, deallylation and final Fmoc removal were performed simultaneously with a solution of 1 equivalent of Pd(Ph3P)4 in THF containing 10% (v/v) piperidine for 3 hours. A chelating wash was performed to remove traces of Pd using 5% (w/v) sodium diethyldithiocarbamate in 5% (v/v) DIPEA in DMF, followed by the normal DMF-DCM-DMF resin wash sequence. The cyclization reaction was performed with 3 equivalents of HATU (Fisher Scientific), 3.2 equiv. HOAT (Fisher Scientific), and 5 equivalents of DIPEA in DMF for 3 hours, followed by resin washing with two final DCM washes to remove residual DMF.

Once compounds 1 and 2 were cyclized, the following procedure was performed for to achieve on-resin N-methylation. This was done using 1 g of resin at a loading of ~0.13 mmol/g of peptide. A solution of lithium *tert*-butoxide (25 ml; 1.5 M) in dry THF was filtered through a 0.2-μ-pore-size filter and then added to the resin. After 30 min the base solution was drained, and without rinsing, a 10% (v/v) solution of methyl iodide in DMSO (25 ml) was added and the resin was agitated for 30 min. The resin was rinsed with water (1 wash), methanol (3 washes), DCM (3 washes), DMF (3 washes) and then DCM (3 washes) again and finally was dried under vacuum.

The peptides that contained side chain protecting groups required a final deprotection that was performed using a solution of 5% (v/v) trimethylsilane in trifluoroacetic acid (TFA) for 1 hour. The cyclic peptides compounds 1 and 2, were finally cleaved from the resin by treating the resin (100 mg) with 5% HF (v/v) in pyridine in THF (5 ml) for 1 hour. The filtrate was collected into a polypropylene tube and the reaction was quenched with 500µl ethoxytrimethylsilane. After evaporation, the peptide was dissolved in acetonitrile (ACN) and H2O (3:1) then purified by reverse-phase preparative HPLC. The solution was then evaporated and the peptide was taken up into a 1:1 solution of water and ACN, it is then flash frozen with liquid nitrogen to yield a solid chunk of ice. The sample was then lyophilized and stored at -20 °C.

PAMPA assay to determine passive membrane diffusion (logP): A 96-well donor plate with 0.45 µm hydrophobic Immobilon-P membrane supports (Millipore) and a 96-well Teflon acceptor plate, were the specialized equipment used in the PAMPA permeability test. The acceptor plate was prepared by adding 300 µL of 5% DMSO/PBS buffer to each well. The compounds to be assayed were prepared as 10 µM solutions in 5% DMSO/PBS buffer, a separate solution was prepared of 1% (w/v) lecithin in dodecane and was sonicated vigourously before use. 5 µL of the lecithin solution was carefully placed via micro-pippette on the artificial membrane supports of the donor plate. Wihtout allowing any of the solution to evaporate, 150 µL of the 10 µM peptide solutions were added to the donor wells. The donor plate

was then placed on top of the acceptor plate so that the artificial membrane in the donor plate came into contact with the buffer solution below in the acceptor well. A lid was then placed on the donor plate and the entire system was covered with a glass evaporating dish and left overnight at room temperature for a period of 12 hours. A wet paper towel was placed inside the system to prevent evaporation and maintain atmospheric equalibrium in the analysis chamber.

Acceptor and donor well concentrations were measured using a (Thermo LTQ) LCMS system using the selective ion monotoring (SIM) mode. An internal standard was prepared using the sidechain protected amino acid H_2N-Tyr(O*t*Bu)-CO_2H, it was run with each sample so that compound-to-standard peak area ratios from (TIC) total ion count detector could be used to accuraly tedetermine concentrations. A 1:3 diltuion of each cyclic peptide 10 μM stock solution was prepared in order to represent the theoretical equilibrium concentration from the PAMPA assay. Next, a solution was prepared containing 90 μL of the theoretical equilibrium mixture, 10 μL of the 10 μM standard, and 90 μL of methanol in a 200 μL LCMS vial insert. 20 μL of this solution was injected in the HPLC –MS and the spectra was recorded. Ratios of analyte-to-standard peak areas were then calculated to represent complete equilibration between donor and acceptor wells (100%T). For the acceptor wells, a solution was prepared by mixing 90 μL of solution taken from the acceptor well after equilibrating for 12 hours, 10 μL of the 10 μM standard soltuion, and as always 90 μL of methanol. This sample was then analyzed via

HPLC-MS to obtain the analyte-to-standard peak area ratio of the system after equilibration for 12 hours. The average compound-to-standard ratio of three acceptor well replicates was divided by the compound-to-standard ratio at equilibrium to obtain the final %T values.

Prior to running the PAMPA a serial dilution of compound 1 was analyzed by LCMS to determine the detection limit of the assay. In general for these cyclic peptides, reliable and quantitative detection was achieved down to 250 pM, representing a detection limit of 0.8% T. To determine the dynamic range of our PAMPA protocol, a dilution series of compound 1 was prepared. Starting with the equilibrium solution, 1:1 dilutions were made using 5% DMSO in PBS buffer solution. These diltuions were then prepared as were the other samples, combining 90 μL of the peptide solution, 90 μL of methanol, and 5 μL of tyrosine tert-butyl ether in methanol standard in a 200 μL polypropylene vial insert. The samples were analyzed using the same instrumental methods as before with 20 μL injection volumes, the TIC HPLC-MS spectra were obtained. Peaks that were burried in the baseline noise corresponded to permeability values that are at the lower limit of detection for this assay which is 0.8% T.

NMR spectroscopy and cyclic peptide structure determination: All NMR spectra were recorded at 297 K on a 600 MHz Varian Inova spectometer equiped with a 5mm inverse detection cryo-probe. All spectra were referenced to residual solvent

proton and carbon resonance signals (δ_H 7.26 , δ_C 77.0 for $CDCl_3$), and were processed using MestReNova (Mestrelab) on a Mackintosh G5 desktop computer. Assignment of resonance for each amino acid residue was accomplised by employing ^1H, ^{13}C, gCOSY, HMQC, HMBC, and TOCSY NMR experiments. Each residue was assigned using ^1H chemical shifts and confirmed through COSY and HMQC crosspeaks. Assembly of these individual residues to form the final cyclized structure was accomplished by considering long-range HMBC correlationsfrom both α-protons and Amide protons to adjacent carbonyl carbons, and α-proton to amide proton NOESYcorrelations between adjacent amino acid residues. NOESY correlations were documented for all available signals, and converted to interproton distances using the relaxation matrix analysis of proton 2D NOE spectra from the volume integrals of NOESY spectra. NOESY experiments were performed with a specific mixing time τ_m of 90 ms. NOE build-up curves were constructed to verify that NOE's were within the linear range of the build-up curve, confirming the validity of the initial rate approximation[70].

Structure calculations were performed using the molecular modeling software CYANA. The *J*(NH-Hα) coupling constants were obtained from 1D spectra recorded with 64K complex points and a spectra width of 7804 Hz. The two *J*(NH-Hα) couplings (Leu^1: 9.49 Hz; Leu^4: 9.15 Hz) for compound 1 were converted into dihedral restraints (+/- 15^o) using the Karplus equation[66] and was the used as dihedral angle restraints in CYANA. No dihedral angle restraints were used in the

computation of the structure for compound 4. Upper and lower distance restraints were obtained by adding 10% to the calculated experimental distances for the upper limits and then subtracting 10% off the calculated experimental distances for the lower limit. The final distance matrix was input into CYANA, a simulated annealing computational simulation was performed to calculate 150 structures for each compound. The resulting conformtaions were analyzed for violations of the distance and dihedral restraint violations, producing an acurate three dimensional representation of the cyclic peptide in the form of a (.pdb) protein data base file. An example of this can be seen in Figure 7.

Figure 13: NMR Assignments for Compound 1

Residue	Resonance	δ_H	δ_C, mult.	COSY	HMBC
Leu[1]	CO	-	173.3	-	-
	α	5.09	47.7, CH	Leu[1] NH, β	Leu[1] CO, β, γ; Tyr CO
	β	1.70, 1.79	41.4, CH_2	Leu[1] NH, α	-
	γ	1.54	24.8, CH	-	-
	δ1	0.96	22.7, CH_3	-	-
	δ2	0.96	22.7, CH_3	-	-
	NH	7.5	-	Leu[1] α	Leu[1] α; Tyr CO
D-Leu[2]	CO	-	174.6	-	-
	α	4.96	52.7, CH	D-Leu[2] β	Leu[1] CO; D-Leu[2] NMe, β, γ, CO
	β	1.41, 1.89	37.5, CH_2	D-Leu[2] α	-
	γ	1.55	25.2, CH	-	-
	δ1	1.02	23.2, CH_3	-	-
	δ2	0.95	22.7, CH_3	-	-
	NMe	3.20	31.2, CH_3	-	Leu[1] CO; D-Leu α
Leu[3]	CO	-	169.9	-	-
	α	5.29	55.2, CH	Leu[3] β	D-Leu[2] CO; Leu[3] NMe, CO, β, γ
	β	1.60, 1.98	36.2, CH2	Leu[3] α, γ	-
	γ	1.35	25.1, CH	Leu[3] β, δ1, δ2	-

	δ1	0.87	20.9, CH_3	Leu^3 γ	-
	δ2	0.94	22.7, CH_3	Leu^3 γ	-
	NMe	3.06	30.8, CH_3	-	D-Leu^2 CO; Leu^3 α
Leu^4	CO	-	170.5	-	-
	α	4.89	48.5, CH	Leu^4 NH, β	Leu^3 β, γ, CO
	β	1.59, 1.71	41.8, CH_2	Leu^4 α	-
	γ	1.53	24.9, CH	-	-
	δ1	0.94	22.7, CH_3	-	-
	δ2	0.93	22.7, CH_3	-	-
	NH	6.88	-	Leu^4 α	Leu^3 CO; Leu^4 α
D-Pro^5	CO	-	173.4	-	-
	α	4.37	55.8, CH	D-Pro^5 β	D-Pro^5 CO, β, γ, δ
	β	1.52, 1.77	28.0, CH_2	D-Pro^5 α, γ	D-Pro^5 CO, α, γ, δ
	γ	1.79, 2.09	25.4, CH_2	D-Pro^5 β, δ	D-Pro^5 α, β, δ
	δ	3.54, 3.77	47.5, CH_2	D-Pro^5 γ	D-Pro^5 α, β, γ
Tyr^6	CO		169.1	-	-
	α	5.67	57.2, CH	Tyr^6 β	D-Pro^5 CO; Tyr^6 CO
	β	2.79, 3.51	32.4, CH_2	Tyr^6 α, β	Tyr^6 CO, α, γ, δ
	γ	-	128.7	-	-
	δ	6.99	129.5, CH	Tyr^6 ε	Tyr^6 δ, ε

ε	6.70	115.1, CH	Tyr^6 δ	Tyr^6 γ, ζ
ζ	-	154.7	-	-
NMe	2.94	31.3, CH_3	-	Tyr^6 α, D-Pro^5 CO

Figure 14: NMR Assignments for Compound 2

Residue	Resonance	δ_H	δ_C, mult.	COSY	HMBC
Leu[1]	CO	-	171.35	-	-
	A	5.48	52.46, CH	Leu1 β	Leu1 CO, β, γ; Tyr CO
	B	1.48, 1.68	38.11, CH_2	Leu1 α, γ	Leu1 CO, α, δ2
	Γ	1.33	28.81, CH	Leu 1 β, δ1	-
	δ1	0.88	45.44, CH_3	-	-
	δ2	1.54	24.67, CH_3	-	-
	NH	2.82	30.69	-	Leu1 α; Tyr CO
D-Leu[2]	CO	-	171.71	-	-
	A	3.48	69.7, CH	Leu2 β	Leu2 CO, β, γ, NMe
	B	1.81, 2.25	38.12, CH_2	Leu2 α, β	Leu2 α, γ, δ1, CO
	Γ	1.44	25.39, CH	-	-
	δ1	0.91	21.96, CH_3	-	-
	δ2	1.69	26.12, CH_3	-	-
	NMe	3.02	38.7, CH_3	-	Leu2 α; Leu1 CO
Leu[3]	CO	-	172.69	-	-
	A	4.77	48.43, CH	Leu3 β, NH	-
	B	1.56, 1.35	41.25, CH2	Leu3 α, γ	-
	Γ	0.89	38.37, CH	Leu3 β	-
	δ1	0.94	23.99, CH_3	-	-

	δ2	-	24.64, CH_3	-	-
	NMe	8.28	-	Pro α	Leu2 CO
Leu[4]	CO	-	169.35	-	-
	A	5.25	51.96, CH	Leu4 β	Leu3 β, γ, CO, NMe
	B	1.07, 1.72	38.25, CH_2	Leu4 α, γ	Leu4 α, δ2
	Γ	1.16	29.51, CH	-	-
	δ1	0.84	18.08, CH_3	-	-
	δ2	0.90	24.20, CH_3	-	-
	NH	2.72	29.65	-	Leu3 CO; Leu4 α
D-Pro[5]	CO	-	172.9	-	-
	A	4.58	56.02, CH	Pro β	-
	B	1.51, 1.88	27.4, CH	Pro α, γ	-
	Γ	1.90, 2.18	38.18, CH_2	Pro β, γ, δ	-
	Δ	3.45, 3.90	46.33, CH_2	Pro γ. δ	-
Tyr[6]	CO		169.8	-	-
	A	5.72	51.47, CH	Tyr β	Tyr CO, β, γ, NMe ; Pro CO
	B	3.06, 2.92	35.13, CH_2	Tyr α, β	Tyr CO, α, γ, δ
	Γ	-	128.24	-	-
	Δ	6.72	129.91, CH	Tyr ε	Tyr ε, ζ
	E	7.06	115.02, CH	Tyr δ	Tyr δ, γ, ζ

Z	-	154.63	-	-
NMe	3.17	29.25	-	Tyr α; Pro CO

Discussion:

The two cyclic peptides, compounds 1 and 2, were the subject of analysis undertaken in this thesis. The three-dimensional models illustrating the conformation of the cyclic peptides, as they exist in a solution of chloroform ($CDCl_3$), are displayed beautifully in Figure 15 using a classic stick diagram to represent the molecules. The stick diagram represents each carbon atom as separate points in the model that are connected by lines that represent the sigma bonds. Hydrogen atoms directly attached to carbon atoms are implied in this diagram, meaning they are not shown, this is true for all of the hydrogen atoms except the ones that are directly involved in a hydrogen-bonding event, which are shown colored white. The oxygen atoms are colored red while the nitrogen atoms are colored blue. The presence of a hydrogen bond is illustrated in the model by a thin red line connecting the two atoms involved in the hydrogen-bonding event. These models beautifully illustrate the complex conformations achieved by these cyclic peptides via transanular hydrogen bonds. These unique conformations allow these molecules to bury their hydrophilic functional groups, by locking them into hydrogen bonds. This results in the

molecules becoming lipophilic enough to become membrane permeable as demonstrated by PAMPA assay results[29].

These structures were produced using simulated annealing, which produces a structure from a given sequence of amino acids in the peptide along with distance restraints derived from 2D NOESY NMR data. These structures provide great insight into the conformational aspects of a molecule that are responsible for lipophilicity and membrane permeability, which are key aspects taken into account when designing new therapeutic agents to be formulated into new drugs or active pharmaceutical ingredients (API). The ability to determine the conformational aspects of large

Figure 15: 3D Conformational Models of Compounds 1 and 2

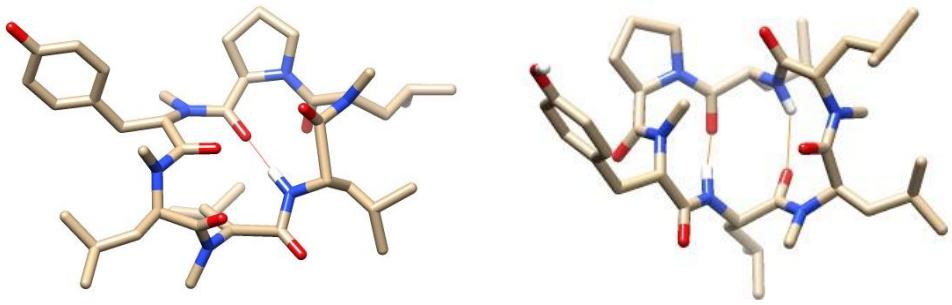

1 2

macrocycles like our cyclic peptides is of great importance to the pharmaceutical research community. These molecules in particular provide a wealth of information about using simple cyclic peptide scaffolds as potential drug candidates by showing the aspects of hydrogen-bonding and backbone methylation patterns that affect the

molecules ability to cross a lipophilic membrane bilayer. This technique provides valuable information that enriches the scientific community as a whole.

References:

1. Johnson, S. M.; Kurtz, M. E., Perceptions of philosophic and practice differences between US osteopathic physicians and their allopathic counterparts. *Social Science & Medicine* **2002,** *55* (12), 2141-2148.

2. Drews, J., Drug Discovery: A Historical Perspective. *Science* **2000,** *287* (5460), 1960-1964.

3. Lam, K. S., New aspects of natural products in drug discovery. *Trends in Microbiology* **2007,** *15* (6), 279-289.

4. Lipinski, C. A., Lead- and drug-like compounds: the rule-of-five revolution. *Drug Discovery Today: Technologies* **2004,** *1* (4), 337-341.

5. Lipinski, C. A.; Lombardo, F.; Dominy, B. W.; Feeney, P. J., Experimental and computational approaches to estimate solubility and permeability in drug discovery and development settings. *Advanced Drug Delivery Reviews* **1997,** *23* (1–3), 3-25.

6. Maggon, K., Best-selling human medicines 2002-2004. *Drug Discovery Today* **2005,** *10* (11), 739-742.

7. Newman, D. J.; Cragg, G. M.; Snader, K. M., Natural Products as Sources of New Drugs over the Period 1981−2002. *Journal of Natural Products* **2003,** *66* (7), 1022-1037.

8. Sarker, S. D.; Latif, Z.; Gray, A. I., Natural product isolation. *Natural Products Isolation, ed. SD Sarker, Z. Latif and AI Gray, 2nd edn, Humana Press, Totowa, New Jersey* **2006**, 1-25.

9. Harvey, A., Strategies for discovering drugs from previously unexplored natural products. *Drug Discovery Today* **2000,** *5* (7), 294-300.

10. Wenger, R. M., Synthesis of Cyclosporine and Analogues: Structural Requirements for Immunosuppressive Activity. *Angewandte Chemie International Edition in English* **1985,** *24* (2), 77-85.

11. Wenger, R., Cyclosporine and analogues--isolation and synthesis--mechanism of action and structural requirements for pharmacological activity. *Fortschritte der Chemie organischer Naturstoffe. Progress in the chemistry of organic natural products. Progrès dans la chimie des substances organiques naturelles* **1986,** *50*, 123.

12. Cheng, W. P.; Gray, A. I.; Tetley, L.; Hang, T. L. B.; Schätzlein, A. G.; Uchegbu, I. F., Polyelectrolyte nanoparticles with high drug loading enhance the oral uptake of hydrophobic compounds. *Biomacromolecules* **2006,** *7* (5), 1509-1520.

13. Hatton, J.; Rosbolt, B.; Empey, P.; Kryscio, R.; Young, B., Dosing and safety of cyclosporine in patients with severe brain injury. *Journal of neurosurgery* **2008,** *109* (4), 699.

14. Haviv, F.; Fitzpatrick, T. D.; Swenson, R. E.; Nichols, C. J.; Mort, N. A.; Bush, E. N.; Diaz, G.; Bammert, G.; Nguyen, A., Effect of N-methyl substitution of the peptide bonds in luteinizing hormone-releasing hormone agonists. *Journal of Medicinal Chemistry* **1993,** *36* (3), 363-369.

15. Chatterjee, J.; Gilon, C.; Hoffman, A.; Kessler, H., N-Methylation of Peptides: A New Perspective in Medicinal Chemistry. *Accounts of Chemical Research* **2008,** *41* (10), 1331-1342.

16. Craik, D. J.; Simonsen, S.; Daly, N. L., The cyclotides: novel macrocyclic peptides as scaffolds in drug design. *Current opinion in drug discovery & development* **2002,** *5* (2), 251-260.

17. Lambert, J. N.; Mitchell, J. P.; Roberts, K. D., The synthesis of cyclic peptides. *Journal of the Chemical Society, Perkin Transactions 1* **2001,** (5), 471-484.

18. Craik, D. J.; Clark, R. J.; Daly, N. L., Potential therapeutic applications of the cyclotides and related cystine knot mini-proteins. *Expert Opinion on Investigational Drugs* **2007,** *16* (5), 595-604.

19. Rizo, J.; Gierasch, L. M., Constrained peptides: models of bioactive peptides and protein substructures. *Annual review of biochemistry* **1992,** *61* (1), 387-416.

20. Witherup, K. M.; Bogusky, M. J.; Anderson, P. S.; Ramjit, H.; Ransom, R. W.; Wood, T.; Sardana, M., Cyclopsychotride A, a Biologically Active, 31-Residue

Cyclic Peptide Isolated from Psychotria longipes. *Journal of Natural Products* **1994,** *57* (12), 1619-1625.

21. König, G. M.; Kehraus, S.; Seibert, S. F.; Abdel-Lateff, A.; Müller, D., Natural products from marine organisms and their associated microbes. *ChemBioChem* **2006,** *7* (2), 229-238.

22. Wang, G., Diversity and biotechnological potential of the sponge-associated microbial consortia. *Journal of industrial microbiology & biotechnology* **2006,** *33* (7), 545-551.

23. Chen, S. H.; Rodriguez, M., Antifungal lipopeptides: a tale of pseudomycin prodrugs and analogues. *Drugs of the Future* **2003,** *28* (5), 441-463.

24. Rinehart Jr, K. L.; Gloer, J. B.; Wilson, G. R.; Hughes Jr, R.; Li, L.; Renis, H.; McGovren, J. In *Antiviral and antitumor compounds from tunicates*, 1983; p 87.

25. Li, P.; Roller, P. P., Cyclization strategies in peptide derived drug design. *Current topics in medicinal chemistry* **2002,** *2* (3), 325-341.

26. Bunnett, N. W., Postsecretory metabolism of peptides. *American Journal of Respiratory and Critical Care Medicine* **1987,** *136* (6 Pt 2), S27-S34.

27. Wade, D.; Boman, A.; Wåhlin, B.; Drain, C.; Andreu, D.; Boman, H. G.; Merrifield, R. B., All-D amino acid-containing channel-forming antibiotic peptides. *Proceedings of the National Academy of Sciences* **1990,** *87* (12), 4761.

28. Rezai, T.; Bock, J. E.; Zhou, M. V.; Kalyanaraman, C.; Lokey, R. S.; Jacobson, M. P., Conformational Flexibility, Internal Hydrogen Bonding, and Passive Membrane Permeability: Successful in Silico Prediction of the Relative Permeabilities of Cyclic Peptides. *Journal of the American Chemical Society* **2006,** *128* (43), 14073-14080.

29. White, T. R.; Renzelman, C. M.; Rand, A. C.; Rezai, T.; McEwen, C. M.; Gelev, V. M.; Turner, R. A.; Linington, R. G.; Leung, S. S. F.; Lokey, R. S.; . On-resin N-methylation of cyclic peptides for discovery of orally bioavailable scaffolds. *Nature Chemical Biology* **2011,** *7* (11), 810-817.

30. Lipinski, C. A., Drug-like properties and the causes of poor solubility and poor permeability. *Journal of pharmacological and toxicological methods* **2000,** *44* (1), 235-249.

31. Conradi, R. A.; Hilgers, A. R.; Ho, N. F. H.; Burton, P. S., The influence of peptide structure on transport across Caco-2 cells. II. Peptide bond modification which results in improved permeability. *Pharmaceutical research* **1992,** *9* (3), 435-439.

32. Rezai, T.; Yu, B.; Millhauser, G. L.; Jacobson, M. P.; Lokey, R. S., Testing the conformational hypothesis of passive membrane permeability using synthetic cyclic peptide diastereomers. *Journal of the American Chemical Society* **2006,** *128* (8), 2510-2511.

33. Loo, J. A.; Loo, R. R. O.; Udseth, H. R.; Edmonds, C. G.; Smith, R. D., Solvent-induced conformational changes of polypeptides probed by electrospray-ionization mass spectrometry. *Rapid Communications in Mass Spectrometry* **1991,** *5* (3), 101-105.

34. Wüthrich, K., Protein structure determination in solution by NMR spectroscopy. *Journal of Biological Chemistry* **1990,** *265* (36), 22059-22062.

35. Smyth, M.; Martin, J., x Ray crystallography. *Molecular Pathology* **2000,** *53* (1), 8-14.

36. Caffrey, M., Membrane protein crystallization. *Journal of Structural Biology* **2003,** *142* (1), 108-132.

37. Wagner, G.; Hyberts, S. G.; Havel, T. F., NMR structure determination in solution: a critique and comparison with X-ray crystallography. *Annual review of biophysics and biomolecular structure* **1992,** *21* (1), 167-198.

38. Uversky, V. N.; Narizhneva, N. V.; Kirschstein, S. O.; Winter, S.; Löber, G., Conformational transitions provoked by organic solvents in [beta]-lactoglobulin: can a molten globule like intermediate be induced by the decrease in dielectric constant? *Folding and design* **1997,** *2* (3), 163-172.

39. Fernández, C.; Wüthrich, K., NMR solution structure determination of membrane proteins reconstituted in detergent micelles. *FEBS Letters* **2003,** *555* (1), 144-150.

40. Crews, P.; Rodriquez, J.; Jaspars, M.; Crews, R. J., *Organic structure analysis*. Oxford New York: 1998; Vol. 23.

41. Englander, S.; Mayne, L.; Bai, Y.; Sosnick, T., Hydrogen exchange: The modern legacy of Linderstrøm-Lang. *Protein science* **1997,** *6* (5), 1101-1109.

42. Toske, S. G.; Cooper, S. D.; Morello, D. R.; Hays, P. A.; Casale, J. F.; Casale, E., Neutral heroin impurities from tetrahydrobenzylisoquinoline alkaloids. *Journal of forensic sciences* **2006,** *51* (2), 308-320.

43. Neuhaus, D., *Nuclear Overhauser Effect*. Wiley Online Library: 2000.

44. Levitt, M. H., *Spin dynamics*. John Wiley & Sons : Chichester, UK: 2001.

45. Claridge, T. D. W., *High-resolution NMR techniques in organic chemistry*. Pergamon Pr: 1999; Vol. 19.

46. Braun, W.; Gō, N., Calculation of protein conformations by proton-proton distance constraints: A new efficient algorithm. *Journal of Molecular Biology* **1985,** *186* (3), 611-626.

47. Herrmann, T.; Güntert, P.; Wüthrich, K., Protein NMR structure determination with automated NOE-identification in the NOESY spectra using the new software ATNOS. *Journal of biomolecular NMR* **2002,** *24* (3), 171-189.

48. Fröhlich, H.; Allemagne, G. B.; Physicist, B.; Germany, G. B., *Theory of dielectrics: dielectric constant and dielectric loss*. Clarendon Press: 1949.

49. Honig, B. H.; Hubbell, W. L.; Flewelling, R. F., Electrostatic interactions in membranes and proteins. *Annual review of biophysics and biophysical chemistry* **1986,** *15* (1), 163-193.

50. Camenisch, G.; Alsenz, J.; van de Waterbeemd, H.; Folkers, G., Estimation of permeability by passive diffusion through Caco-2 cell monolayers using the drugs' lipophilicity and molecular weight. *European journal of pharmaceutical sciences* **1998,** *6* (4), 313-319.

51. Brünger, A. T.; Clore, G. M.; Gronenborn, A. M.; Karplus, M., Three-dimensional structure of proteins determined by molecular dynamics with interproton distance restraints: application to crambin. *Proceedings of the National Academy of Sciences* **1986,** *83* (11), 3801.

52. Berman, H. M.; Westbrook, J.; Feng, Z.; Gilliland, G.; Bhat, T.; Weissig, H.; Shindyalov, I. N.; Bourne, P. E., The protein data bank. *Nucleic acids research* **2000,** *28* (1), 235-242.

53. DeLano, W. L., The PyMOL molecular graphics system. **2002**.

54. Pettersen, E. F.; Goddard, T. D.; Huang, C. C.; Couch, G. S.; Greenblatt, D. M.; Meng, E. C.; Ferrin, T. E., UCSF Chimera—a visualization system for exploratory research and analysis. *Journal of computational chemistry* **2004,** *25* (13), 1605-1612.

55. Guntert, P., Automated NMR structure calculation with CYANA. *METHODS IN MOLECULAR BIOLOGY-CLIFTON THEN TOTOWA*- **2004,** *278*, 353-378.

56. Szyperski, T.; Güntert, P.; Otting, G.; Wüthrich, K., Determination of scalar coupling constants by inverse Fourier transformation of in-phase multiplets. *Journal of Magnetic Resonance (1969)* **1992,** *99* (3), 552-560.

57. Weil, J. A.; Bolton, J. R., *Electron paramagnetic resonance: elementary theory and practical applications*. Wiley: 2007.

58. Kuwata, K.; Matumoto, T.; Cheng, H.; Nagayama, K.; James, T. L.; Roder, H., NMR-detected hydrogen exchange and molecular dynamics simulations provide structural insight into fibril formation of prion protein fragment 106–126. *Proceedings of the National Academy of Sciences* **2003,** *100* (25), 14790.

59. Wagner, G.; Pardi, A.; Wuethrich, K., Hydrogen bond length and proton NMR chemical shifts in proteins. *Journal of the American Chemical Society* **1983,** *105* (18), 5948-5949.

60. Gippert, G. P.; Yip, P. F.; Wright, P. E.; Case, D. A., Computational methods for determining protein structures from NMR data. *Biochemical pharmacology* **1990,** *40* (1), 15-22.

61. Kumar, A.; Wagner, G.; Ernst, R. R.; Wuethrich, K., Buildup rates of the nuclear Overhauser effect measured by two-dimensional proton magnetic resonance spectroscopy: implications for studies of protein conformation. *Journal of the American Chemical Society* **1981,** *103* (13), 3654-3658.

62. Bode, W.; Turk, D.; Karshikov, A., The refined 1.9-Å X-ray crystal structure of d-Phe-Pro-Arg chloromethylketone-inhibited human α-thrombin: Structure analysis, overall structure, electrostatic properties, detailed active-site geometry, and structure-function relationships. *Protein science* **1992,** *1* (4), 426-471.

63. Dilger, J. P.; McLaughlin, S.; McIntosh, T. J.; Simon, S. A., The dielectric constant of phospholipid bilayers and the permeability of membranes to ions. *Science* **1979,** *206* (4423), 1196-1198.

64. Uematsu, M.; Franck, E., *Static dielectric constant of water and steam*. American Chemical Society and the American Institute of Physics for the National Bureau of Standards: 1981.

65. McElhearn, K., SECRETS-GEEK FACTOR-Take Control of Text-Bare Bones Software's free TextWrangler offers the power of a command-line text editor in a nice interface. Learn-what tricks this program can do. *Macworld-Boulder* **2005**, 84-87.

66. Ludvigsen, S.; Andersen, K. V.; Poulsen, F. M., Accurate measurements of coupling constants from two-dimensional nuclear magnetic resonance spectra of proteins and determination of [phi]-angles. *Journal of Molecular Biology* **1991,** *217* (4), 731-736.

67. Merrifield, B., Solid-phase peptide synthesis. *Peptides: synthesis, structures, and applications* **1995**, 94-169.

68. Dean, T., A Practical Introduction to Solid Phase Chemistry. GlaxoWelcome R&D: 1998.

69. Fuentes, G.; Hood, C.; Park, J. H.; Patel, H.; Page, K.; Menakuru, M., Fast Conventional Synthesis of Human ß-Amyloid (1–42) on the Symphony® and Prelude™. *Peptides for Youth* **2009**, 173-174.

70. Hu, H.; Krishnamurthy, K., Revisiting the initial rate approximation in kinetic NOE measurements. *Journal of Magnetic Resonance* **2006,** *182* (1), 173-177.